

PCCP

Accepted Manuscript



This is an *Accepted Manuscript*, which has been through the Royal Society of Chemistry peer review process and has been accepted for publication.

Accepted Manuscripts are published online shortly after acceptance, before technical editing, formatting and proof reading. Using this free service, authors can make their results available to the community, in citable form, before we publish the edited article. We will replace this *Accepted Manuscript* with the edited and formatted *Advance Article* as soon as it is available.

You can find more information about *Accepted Manuscripts* in the [Information for Authors](#).

Please note that technical editing may introduce minor changes to the text and/or graphics, which may alter content. The journal's standard [Terms & Conditions](#) and the [Ethical guidelines](#) still apply. In no event shall the Royal Society of Chemistry be held responsible for any errors or omissions in this *Accepted Manuscript* or any consequences arising from the use of any information it contains.

Aqueous solvation of amphiphilic molecules by extended depolarized light scattering: The case of trimethylamine-N-oxide.

L. Comez^{1,2*}, M. Paolantoni³, S. Corezzi², L. Lupi⁴, P. Sassi³, A. Morresi³, and D. Fioretto^{2,5}

¹*IOM-CNR c/o Dipartimento di Fisica e Geologia, Università di Perugia, Via Pascoli, I-06123 Perugia, Italy*

²*Dipartimento di Fisica e Geologia, Università di Perugia, Via Pascoli, I-06123 Perugia, Italy*

³*Dipartimento di Chimica, Biologia e Biotecnologie, Università di Perugia, Via Elce di Sotto 8, I-06123 Perugia, Italy*

⁴*Department of Chemistry, The University of Utah, 315 South 1400 East, Salt Lake City, Utah 84112-0850, United States*

⁵*Centro di Eccellenza sui Materiali Innovativi Nanostrutturati (CEMIN), Università di Perugia, Via Elce di Sotto 8, I-06123 Perugia, Italy*

ABSTRACT

Hydrophilic and hydrophobic interactions strongly affect the solvation dynamics of biomolecules. To understand their role, small model systems are generally employed to simplify the investigations. In this study the amphiphile trimethylamine N-oxide (TMAO) is chosen as exemplar, and studied by means of extended frequency range depolarized light scattering (EDLS) experiments as a function of solute concentration. This technique proves to be a suitable tool for investigating different aspects of aqueous solvation, being able at the same time to provide information about relaxation processes and vibrational modes of solvent and solute. For the case study TMAO, we find that the relaxation dynamics of hydration water is moderately retarded with respect to the bulk, and the perturbation induced by solute on surrounding water is confined to the first hydration shell. The results highlight the hydrophobic character of TMAO in its interaction with water. The number of molecules taking part in the solvation process decreases as the solute concentration increases, following a trend consistent with the hydration water-sharing model, and suggesting that aggregation between solute molecules is negligible. Finally, the analysis of the resonant modes in the THz region, and the comparison with corresponding results for the

isosteric molecule *tert*-butyl alcohol (TBA) allow us to provide new insights into the different solvating properties of these two biologically relevant molecules.

I. INTRODUCTION

Understanding the role played by hydrophilic and hydrophobic interactions in the solvation dynamics of biomolecules is important in a variety of phenomena, from membrane assembling to protein-ligand binding and protein folding.¹ The choice of small amphiphilic systems has occasionally proved to be ingenious because it allows one to simplify the problem.² Trimethylamine N-oxide (TMAO) and *tert*-butyl alcohol (TBA) are among the most widely used model systems for studying the effects of hydrophobic solutes in water, such as hydrophobic hydration and hydrophobic interaction.^{3,4,5,6} Although the results obtained on such small model molecules cannot be trivially extended to the hydrophobic hydration of larger molecules,² it has to be noted that TMAO and TBA and the perturbation they induce on surrounding water are interesting per se, due to the relevance of these molecules as cosolutes in biological aqueous solutions.⁷ In fact, the first compound is a potent osmolyte, which is known to enhance thermodynamic stability of proteins and protect them against denaturation;^{8,9,10,11} the second one is a denaturant, showing a destabilising effect upon the native conformation of proteins.¹² TMAO and TBA exhibit a similar chemical structure having tetrahedral geometry, with the same hydrophobic part (consisting of three methyl groups) and a different hydrophilic head (a polar N^+O^- group and a hydroxyl group, respectively). Despite the similarities in their structure, these solutes behave quite differently in aqueous solution, and in particular, TBA tends to associate whereas TMAO does not.^{13,14,15}

A fundamental question that needs to be clarified is to what extent the structure and dynamics of interfacial water is perturbed by these small molecules. Most of the studies have not found evidence that the structure of water surrounding hydrophobic groups is different from bulk liquid water, that is, liquid water can accommodate for a small hydrophobe without modifying its structural properties.^{16,17,18} The dynamics, however, is effectively affected by hydrophobic hydration. In this regard, the literature presents different estimates for the dynamical retardation between hydration and bulk water (ξ) and for the percentage of solvent molecules involved in the solvation process.^{14,19,20,21,22,23,24}

Several techniques indicate that the presence of hydrophobic groups in small amphiphiles is the main cause of changes in the rotational and translational dynamics of hydrating water molecules.^{24,25,26,27,28,29} However, they provide conflicting results: polarization and time-

resolved infrared experiments detect a pronounced slowdown ($\xi > 4$) of few water molecules in the hydration shell of TMAO,^{28,29} in agreement with 2D-IR experiments that reveal considerably slower dynamics of the O–H stretching vibration ratio for HDO molecules solvating amphiphilic molecules;^{13,19} on the other hand, molecular dynamics (MD) simulations, Nuclear magnetic resonance (NMR) and Brillouin light scattering (BLS) experiments observe that hydrophobic groups slow down to a minor extent ($\xi \leq 2$) the dynamics of all the water molecules belonging to the first hydration shell.^{14,24,25,26} Moreover, broadband dielectric experiments find that a small number of solvating water molecules (5-9) are slowed down by a factor $\xi \sim 2-3$,³⁰ and studies of THz dynamics by ultrafast optical Kerr effect also report a retardation factor of about 2–3 only for some thirty molecules in the hydration shell.^{31,32} In summary, a very uneven picture of solvation properties emerges from the literature.

In this context, it has to be noted that frequently, due to the restricted frequency range covered by single experiments, the estimates of the retardation factor and hydration number are made separately and/or they require some parameter to be fixed during data analysis. Giving the experiments a wider spectral extension is therefore important to carry out a simultaneous determination of these two quantities. Here we report on the use of extended frequency range depolarized light scattering (EDLS), an extended version of conventional techniques like Brillouin and Raman light scattering, which allows us to study simultaneously various features of aqueous solutions, from relaxation processes (in the GHz region) to vibrational modes of solvent and solute (in the THz region). Solutes that have been so far investigated by our group differ in size and complexity, spanning from small hydrophilic molecules such as carbohydrates, to amphiphilic amino acids and peptides,^{33,34,35,36,37} up to more complex systems such as proteins.^{38,39,40} Very recently, we have applied EDLS to study TBA/water solutions,⁴¹ and found that solute-solvent contacts are mediated by hydrophobic interactions, which are responsible for a moderate slowing down ($\xi \sim 4$) of water molecules in the first hydration shell. The decrease of hydration numbers on increasing TBA concentration has been recognized to be a sign of TBA-TBA aggregation phenomena. In the present paper, we report on the study of TMAO/water solutions, and discuss the different solvation properties with respect to TBA.

II. EXPERIMENT

EDLS experiments were performed on TMAO/water solutions at $T = 20^\circ\text{C}$, in the range $0 < x < 0.05$ of solute molar fraction. In addition, low-wavenumber Raman scattering experiments were carried out at the same temperature, for solute molar fractions up to $x = 0.1$. TMAO was purchased by Sigma-Aldrich with purity $> 99\%$ and dissolved without further purification into doubly distilled deionized water. Freshly prepared solutions were directly poured into the optical quartz cell through filters with a $0.2\ \mu\text{m}$ pore size. Depolarized spectra (I_{VH}) were collected in the frequency range between 0.3 GHz and 30 THz making use of two different spectrometers: a Sandercock-type (3+3)- pass tandem Fabry - Perot interferometer⁴² in the range 0.3-200 GHz, and an ISA Jobin-Yvon model U1000 double monochromator in the range 3 GHz - 30 THz. The spectral profiles were spliced over a wide overlapping region,³⁵ and the imaginary part $\chi''(\omega)$ of the susceptibility spectrum was calculated as the ratio between $I_{VH}(\omega)$ and $[n(\omega)+1]$, where $n(\omega)$ is the Bose - Einstein occupation number, i.e. $n(\omega) = 1/[\exp(h\omega/k_B T) - 1]$

III. RESULTS AND DISCUSSION

The susceptibility spectra of water and TMAO/water solutions are reported in Fig. 1. The spectrum of pure water is used as a comparison to the spectra of solutions. It is characterized by different spectral components, whose origin has already been discussed in literature. The bump at some hundreds of GHz arises from the structural relaxation of water,⁴³ a process of translational nature related to fast restructuring of the H-bond network.^{44,45,46} The high frequency (THz) region of the spectrum is characterized by two distinct peaks attributed to the H-bond intermolecular bending (1.5 THz) and stretching (5.1 THz) Raman modes.⁴⁷ Librational modes of water molecules give rise to an additional broad asymmetric peak at even higher frequencies (10-30 THz). This feature, generally not much influenced by the addition of solute or by temperature changes, is used to normalize the spectra of the solutions,^{35,48,49} and to calculate the solvent free spectra (χ''_{SF}) by subtracting the spectral profile of pure water from those of the solutions (see bottom panel of Fig. 1).

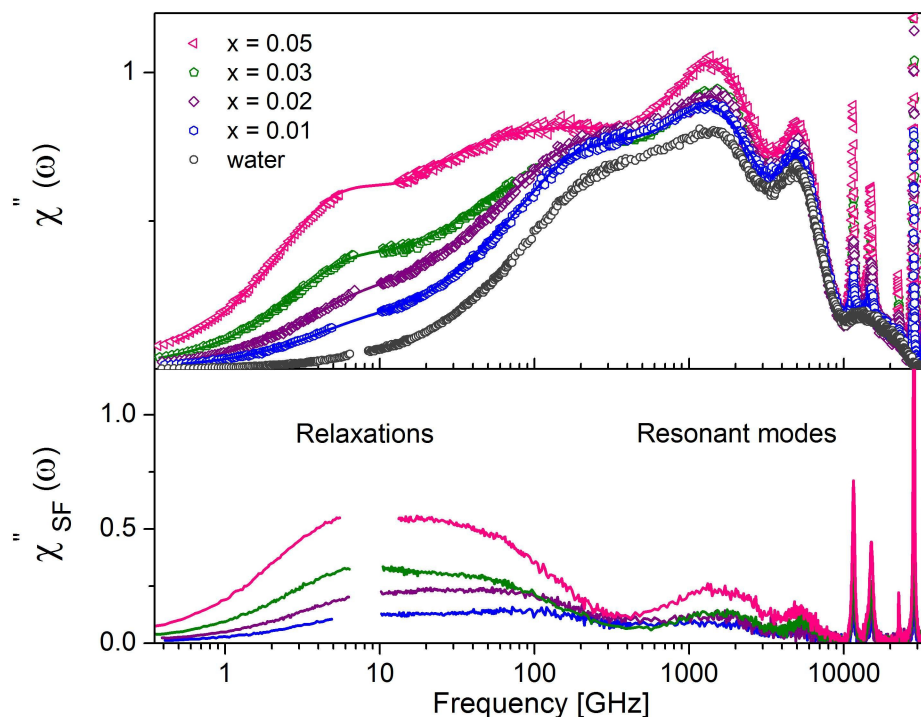


Fig. 1 Top: EDLS susceptibility (symbols) of water and TMAO/water solutions at different concentrations, at $T=20$ °C. The solid lines represent the fitting curves described in the text, the gap in the low frequency part of EDLS spectrum is due to the removal of few spurious points originated by the leakage of the Brillouin peaks. Bottom: Solvent free spectra obtained by subtracting the spectral profile of pure water to those of solutions.

From a qualitative point of view, EDLS spectra result to be strongly affected by the addition of solute, even at the lowest concentration investigated, showing a substantial increase of intensity as the concentration increases (Fig. 1). The removal of the solvent contribution help visualize the main spectral changes induced by the presence of the solute: residual features are indeed detected in the low frequency (relaxations) and in the high frequency (resonant modes) region. In particular, in the region from fraction to hundred GHz (see bottom panel of Fig. 1), χ''_{SF} allows us to appreciate the presence of a wide spectral band. On the basis of information from other bio-systems,^{33,34,35,36,37,38,39} it is reasonable to suppose that this band arises from two spectral contributions: one around 5 GHz originating from the rotational diffusion of solute molecules,^{35,49,50,51} and the other around 50 GHz due to the translational dynamics of solvating water molecules.³⁶ The remaining part of the spectrum in the THz region is, instead, associated to resonant modes of water and/or TMAO.

Consistently with previous studies, we confirm these assumptions and get quantitative information about the dynamical processes probed by EDLS by modeling the EDLS

susceptibility with the following phenomenological function, able to reproduce the whole spectral profile:

$$\chi''_{EDLS}(\omega) = \text{Im} \left\{ -\Delta_{TMAO} [1 + i\omega\tau_{TMAO}]^{-1} - \Delta_{hydr} [1 + i\omega\tau_{hydr}]^{-\beta_{hydr}} - \Delta_{bulk} [1 + i\omega\tau_{bulk}]^{-\beta_{bulk}} + \Delta_b \omega_b^2 [\omega^2 - \omega_b^2 - i\omega\Gamma_b]^{-1} + \Delta_s \omega_s^2 [\omega^2 - \omega_s^2 - i\omega\Gamma_s]^{-1} \right\} \quad [1]$$

The relaxation part of this expression is given by the sum of a Debye function for the rotational diffusion of TMAO and two Cole–Davidson relaxation functions for the bulk-like and hydration water components, where Δ_{TMAO} is the amplitude, and τ_{TMAO} the characteristic time of TMAO rotational diffusion, Δ_{hydr} , τ_{hydr} , β_{hydr} and Δ_{bulk} , τ_{bulk} , β_{bulk} are, respectively, the amplitude, characteristic time and shape parameter for the two relaxation processes of water. The shape of the spectrum in the THz region, due to solute and/or solvent resonant modes, is effectively reproduced by two damped harmonic oscillator functions.⁴¹ Concerning the shape of water relaxations, we recall that the use of a Cole-Davidson function to describe anisotropy fluctuations of bulk water in the frequency domain (stretched exponential in the time domain) is well documented in the literature.⁵² As shown in the supporting material,[†] there are quantitative arguments sustaining the choice of using the same phenomenological function to model the relaxation assigned to hydration water. According to this modeling, average relaxation times $\langle \tau_{hydr} \rangle = \beta_{hydr} \tau_{hydr}$ and $\langle \tau_{bulk} \rangle = \beta_{bulk} \tau_{bulk}$ are obtained for hydration and bulk water, respectively. During the fitting session, in order to reduce the number of free fitting parameters, β_{hydr} and β_{bulk} are fixed to the value 0.6,[†] as obtained in pure water.^{35,52}

III.1 Relaxations

Hydration and bulk water relaxations. The ability of EDLS to simultaneously provide the dynamical retardation factor and the number of water molecules affected by the solute, relies on the assumption that the relaxation contribution to the spectrum can be described as the sum of separate features assigned to solute, bulk and hydration water. This basic assumption, successfully tested by MD simulations on carbohydrates aqueous solution,^{34,53} and effectively applied to other small molecules such as *tert*-butyl alcohol⁴¹ and levoglucosan,⁴⁹ is also applied to the present case. We recall that, to experimentally discern two separate water contributions the probing technique has to be faster than the time needed to water molecules

to exchange from the bulk to the hydration environment. Exchange times longer than tens of ps can be inferred for TMAO and other similar solutes, demonstrating that EDLS reasonably fulfills the required “slow exchange” condition.⁴¹ Moreover, it should be noted that for the observed water relaxation processes (10-100 GHz) the most important contribution to the scattering cross-section arises from fluctuations of intermolecular distances activated by the dipole-induced dipole effect,⁴⁵ and therefore the obtained two relaxation processes get their strength from local translations of water molecules.

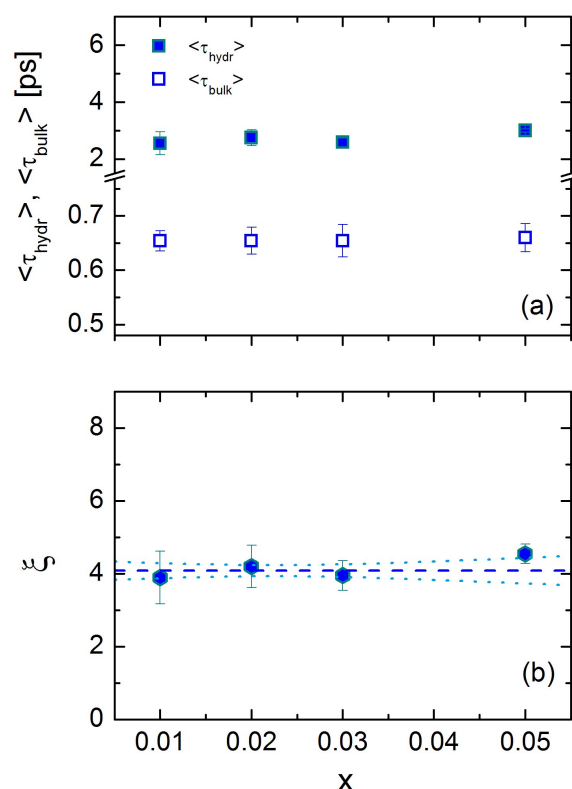


FIG. 2 (a) Average relaxation time of bulk ($\langle \tau_{bulk} \rangle$) and hydration ($\langle \tau_{hydr} \rangle$) water for TMAO/water solutions and (b) retardation ratio $\xi = \langle \tau_{hydr} \rangle / \langle \tau_{bulk} \rangle$ as a function of solute molar fraction, at $T = 20$ °C. The result of a linear regression procedure (dashed line) to the experimental data and the corresponding 68% confidence bands (dotted lines) are also reported in the panel (b).

The fitting results for the average relaxation times obtained from Eq. 1 are reported in Fig. 2a, revealing a negligible concentration dependence. In particular, at any fixed concentration, we find that $\langle \tau_{bulk} \rangle$ is very close to the relaxation time of pure water observed at the same temperature (0.65 ps at 20°C);⁵⁴ moreover, the relaxation time of hydration water can be easily distinguished from that of bulk water in the whole concentration range. The average relaxation times are then used to calculate the retardation factor $\xi = \langle \tau_{hydr} \rangle / \langle \tau_{bulk} \rangle$. This

parameter turns out to be concentration independent within experimental error, and close to 4 ($\xi = 4.1 \pm 0.1$, see Fig. 2b), which is in agreement with the result obtained by EDLS for TBA ($\xi = 4.1 \pm 0.3$);⁴¹ but different from the case of small hydrophiles, like mono and di-saccharides ($\xi = 5-6$),^{34,53,55} and from the case of peptides and proteins ($\xi = 7-8$).^{35, 36,37,38}

Therefore, although our calculated value of ξ represents an average factor, without being able to discriminate whether the slowdown is uniform at the solute-solvent interface, the common value of ξ for TMAO and TBA suggests that their similar hydrophobic portion could be mainly responsible for the observed dynamical effect on hydration water. The more general result is that TMAO and TBA are less effective in dynamically perturbing the H-bond network of liquid water compared to more complex amphiphilic molecules,^{35,37} in which an interplay between polar and apolar groups causes, on average, a greater modification of the dynamics of surrounding water.³⁶ Moreover, the results of the present analysis also suggest that the dynamics of hydration water is less restricted at the interface of the small hydrophobes TMAO and TBA, compared to the hydrophilic sugars.^{33,34,56} In fact, EDLS also provides a determination of the dynamical hydration number. This is done through the relation $N_{hydr} = \Delta_{hydr} (\Delta_{hydr} + \Delta_{bulk})^{-1} (1-x) x^{-1}$, where Δ_{bulk} and Δ_{hydr} are the peak area corresponding to bulk and hydration water (see Eq. 1), assuming that the amplitude of each relaxation is proportional to the fraction of relaxing water molecules. Table I reports the fitting parameters obtained from the analysis of the spectra.

With respect to the data of Table 1, we want to emphasize two findings which give support to our analysis: First, we note that the total area of the water components, $\Delta_{tot} = \Delta_{bulk} + \Delta_{hydr}$, shows small variations (less than 10%) in the 0.01-0.03 molar fraction range, as already observed in the case of TBA water solutions.⁴¹ This represents an indirect verification that the solute-solvent cross terms in the scattering cross section is not significant and that this latter is basically the same for hydration and bulk water contributions.⁴¹ A larger variation (ca. 30 %) is found for the $x=0.05$ solution, likely due to the fact that at this concentration it is more difficult to rescale the spectra on the broad librational band at 10-20 THz due to the relatively higher contributions of solute intramolecular signals in this region. Second, we observe that the ratio $\Delta_{hydr}/\Delta_{tot}$ (last column in Tab. I) provides an estimate of the fraction of hydration water in TMAO solutions which is independent from the adopted normalization, and in line with a geometric calculation of the fraction of interfacial water surrounding TMAO molecules at similar concentrations, as resulting from MD simulations.⁵⁷

x	Δ_{hydr}	Δ_{bulk}	Δ_{tot}	$\Delta_{hydr}/\Delta_{tot}\%$
0.01	0.28 ± 0.04	1.36 ± 0.06	1.64 ± 0.10	17
0.02	0.50 ± 0.04	1.29 ± 0.04	1.79 ± 0.08	28
0.03	0.69 ± 0.04	1.08 ± 0.03	1.77 ± 0.07	39
0.05	1.21 ± 0.06	0.88 ± 0.03	2.09 ± 0.09	58

Tab. I Area of the peaks corresponding to the relaxation of bulk (Δ_{bulk}) and hydration water (Δ_{hydr}), their sum, and the fraction of hydration water molecules in the solution, obtained from the fit of Eq. 1 to the experimental spectra of Fig. 1.

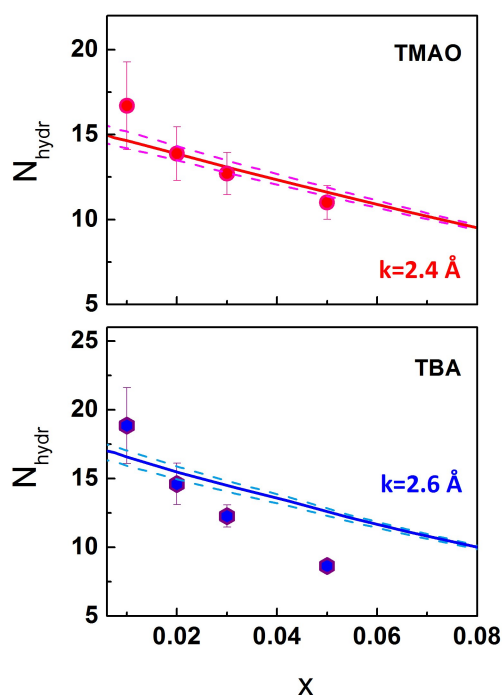


FIG. 3. Average hydration number N_{hydr} calculated from EDLS data as described in the text. The values obtained from the numerical water-sharing model for non-interacting molecules⁵⁸ are also represented (solid line) for comparison. Upper panel: For TMAO, the model provides an effective hydration shell thickness equal to $k=2.40$ Å (continuous red line). Dashed lines refer to simulations with $k=2.45$ Å and 2.35 Å, which also well reproduce the experimental data. Bottom panel: For TBA, continuous blue line refers to $k=2.58$ Å, and dashed lines to $k=2.53$ Å and 2.63 Å, details are given in Ref. 41.

Based on these premises, we turn our attention to the decreasing concentration dependence of N_{hydr} , shown in Fig. 3. An explanation of this behavior can be found in the water-sharing phenomenon between hydration shells of close-to-contact solute molecules. To give a quantitative estimation of this effect, we apply a simple numerical model recently developed by our group⁵⁸ representing the solute molecule as a sphere (radius for TMAO

$c=2.64 \text{ \AA}$, in agreement with the estimate of the hydrodynamic volume, $V = 77 \text{ \AA}^3$, discussed in the next paragraph) with an effective hydration shell of constant thickness k .

The method is based on the generation of random distributions of spherical solute molecules in water. Periodic boundary conditions are used for a box filled with water (~27000 molecules) at the proper density, in which solute molecules are randomly placed, at the desired molar ratio. For each resulting configuration, the number of hydration molecules is evaluated as the total number of water molecules that fall within a distance k from the surface of any solute molecule. The experimental N_{hydr} trend is effectively reproduced by the average hydration number obtained with this model using a thickness $k=2.40\pm 0.05 \text{ \AA}$, as reported in Fig. 3 (upper panel). Accordingly, the hydration number for a single TMAO molecule in the infinite dilution limit is obtained: $N_{\text{hydr}}^0 = 15.4\pm 0.5$. This result indicates that TMAO dynamical perturbation falls within the first hydration layer. Indeed, comparable values for hydration numbers are found by other numerical and experimental works.^{3,15,59} Moreover, the good agreement of the model with the data in the whole range of concentrations suggests that the overall decreasing behavior of N_{hydr} can be interpreted just by considering the random close-to-contact condition of solute molecules, without the need to invoke aggregation phenomena between particles.

Comparing the present findings with those obtained for TBA (bottom panel of Fig. 3), it is worth noting that similar values for k and N_{hydr}^0 (for TBA, $k=2.58$ and $N_{\text{hydr}}^0 \sim 17.5$) have been found for the two systems, highlighting an analogous short range perturbation in line with molecular dynamics simulation results.^{15,59} Interestingly, in TBA a definitely steeper trend of N_{hydr} vs x was found by EDLS, which cannot be entirely explained in terms of random overlapping of hydration shells, and suggests a larger propensity of TBA to self-aggregate.⁴¹ Recent findings from Raman and ultrafast infrared experiments, in partial disagreement with the self-aggregation picture, emphasize that the occurrence of solute-solute contacts in TBA solutions is instead essentially random,^{5,60} leaving open some stimulating issues.

Nevertheless, the existence of differences in the aggregation behavior between TBA and TMAO is an established fact. Here we are showing how these differences, already evidenced through the analysis of other structural and dynamical properties,^{4,15,59} also emerge from the concentration dependence of the average number of dynamically perturbed water molecules derived by EDLS experiments, which specifically probe water (translational) rearrangements at the picosecond timescale. Overall, while the different hydrophilic moieties in TMAO and TBA modulate their aggregation tendency, the characteristic average relaxation time of

interfacial water is found to be similarly perturbed by the two molecules, in line with the picture that a dominant fraction of hydration water is interacting with their hydrophobic part. In this regard, it is also worth noticing that the viscosity of TBA/water and TMAO/water solutions shows the same concentration increase in the range $0 < x < 0.05$,⁴ suggesting that the main contribution to the viscosity increase at these concentrations comes from the effect induced by the hydrophobic part on hydration water.^{25,26}

TMAO rotational diffusion. As a broadband technique, EDLS allows us also to obtain information about the relaxation dynamics of solute. Specifically, the lowest frequency contribution described in the previous section, peaked at about 5 GHz, is very well described by a Debye function, whose characteristic time (τ_{TMAO}) is reported in Fig. 2 vs the solute molar fraction x .

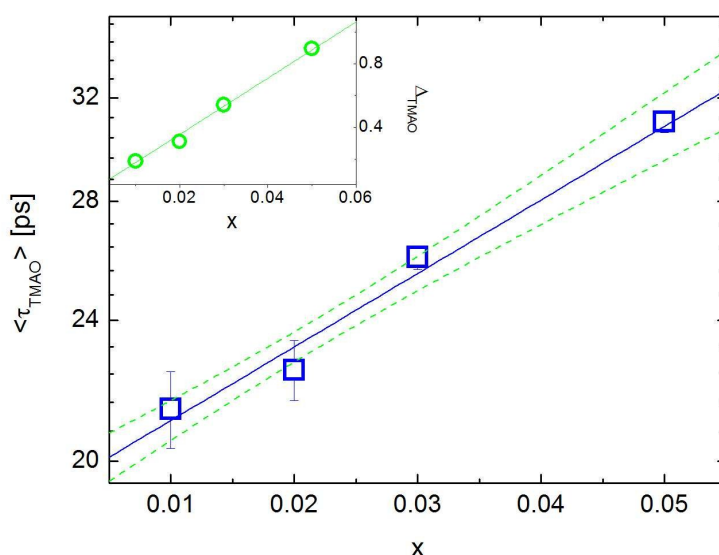


FIG. 4. Rotational relaxation time of TMAO as a function of solute concentration at $T = 20$ °C. The solid line indicates Arrhenius behavior, i.e. the logarithm of the relaxation time is proportional to the solute molar fraction (dashed lines are 68% confidence bands). In the inset, the amplitude of relaxation, Δ_{TMAO} , shows a linear behavior vs the solute molar fraction.

The behavior is well reproduced by an exponential raise: the solid line, together with 68% confidence bands, shows the result of the fitting procedure with an Arrhenius law.⁶¹ Similarly to what found in other aqueous solutions, like sugar^{49,50,51} and peptide-water mixtures,^{35,36} such a behavior can be associated with the exponential increase of viscosity with solute concentration. In addition, we observe that the amplitude of the relaxation process, Δ_{TMAO} , increases proportionally to the increase of solute (inset of Fig. 4).

Our findings suggest that this spectral contribution is associated with the rotational diffusion of solute molecules. Consequently, the Stokes–Einstein–Debye (SED) equation, $\tau_s = V_h \eta / (k_B T)$, connecting the single particle relaxation time τ_s to the volume V_h of the molecule diffusing in a solution of viscosity η , can be applied. To this end, the limit of infinite dilution must be considered. Indeed, in this limit EDLS, which generally measures the collective reorientational relaxation time, provides the single particle correlation time.⁶² We therefore extrapolate the value of $\langle \tau_{\text{TMAO}} \rangle$ to the $x \rightarrow 0$ limit (19.4 ± 0.3 ps), and by using the viscosity of water at 20°C (1.002 cPoise) we obtain $V_h = 77 \pm 3 \text{ \AA}^3$, which is in reasonable agreement with the estimated van der Waals volume of TMAO, $V_{vdW} = 83.6 \text{ \AA}^3$.³⁶ This agreement further supports the spectral decomposition we have made and the assignment of components.

It has to be noted that a TMAO relaxation time of ca. 60 ps has been recently found in broadband dielectric spectroscopy experiments,³⁰ in agreement with previous assignments.^{63,64} This corresponds to a first-order rotational correlation time of 41 ps and to a second-order rotational relaxation time (to be compared to EDLS results) of about 14 ps.³⁰ Such value reasonably agrees with our estimate and also matches the N–O rotational relaxation time (14 ps) derived by MD simulations.¹⁴ The fact that, in the framework of the SED model, comparable hydrodynamic and van der Waals volumes are obtained would imply that, similarly to the case of other hydrogen bonding solutes, the average lifetime of TMAO–water interaction is smaller than the solute rotation. In other words, water molecules do not follow TMAO during its rotational motion.

By contrast, an opposite picture was derived by analyzing the amplitude of different contributions of dielectric spectra in conjunction with quantum mechanical *ab initio* calculations.³⁰ In that case, it was argued that an enhancement of the effective TMAO dipole moment occurs in solution due to the formation of long-lasting TMAO–water complexes involving 2–3 water molecules with characteristic lifetimes exceeding the slow dielectric relaxation time (< 60 ps).³⁰ In this respect, we note that EDLS relaxation times estimated at infinite dilution are practically the same for TBA and TMAO, clearly indicating that the increased tendency of this latter to form strong H-bonds with water through the N–O group does not influence its (small-step) rotational diffusion. On the other hand, these interactions seem to have a role in the higher frequency ultrafast vibrational dynamics, as shown in the next paragraph.

We conclude this section emphasizing that, despite similar viscosity values,⁴ relaxation times are definitively longer in TBA⁴¹ than in TMAO, especially at higher concentrations. This

might be tentatively attributed to the enhanced tendency of TBA to aggregate, which could be reflected in increased solute-solute cross-term correlations at higher concentrations.

III.2 Resonant modes

The study of the low frequency region of Raman spectra ($10\text{-}350\text{ cm}^{-1}$), related to intermolecular modes, enables us to gain significant information about changes on solute-induced intermolecular interactions. In detail, Fig. 5(a) shows depolarized Raman spectra of water/TMAO solutions at different solute molar fractions, ranging from $x=0.01$ to $x=0.1$. The spectrum of pure water is also reported, showing its distinctive contributions arising from intermolecular bending (60 cm^{-1}) and stretching (180 cm^{-1}) modes, together with a broad librational feature ($300\text{-}900\text{ cm}^{-1}$) used to normalize the spectra.^{37,48,49} This latter contribution appears as a spectral background in the signal from the solutions, below several sharp intramolecular peaks. The addition of solute progressively causes changes in the spectrum, and particular attention has been given to the analysis of the spectral window from 15 to 330 cm^{-1} , which is framed by a rectangle in Fig. 5 (a). Differences with pure water can be better appreciated by observing the solvent free spectra, χ''_{SF} , reported in Fig. 5(b); similar spectra have been previously obtained in the case of TBA/water solutions.⁴¹

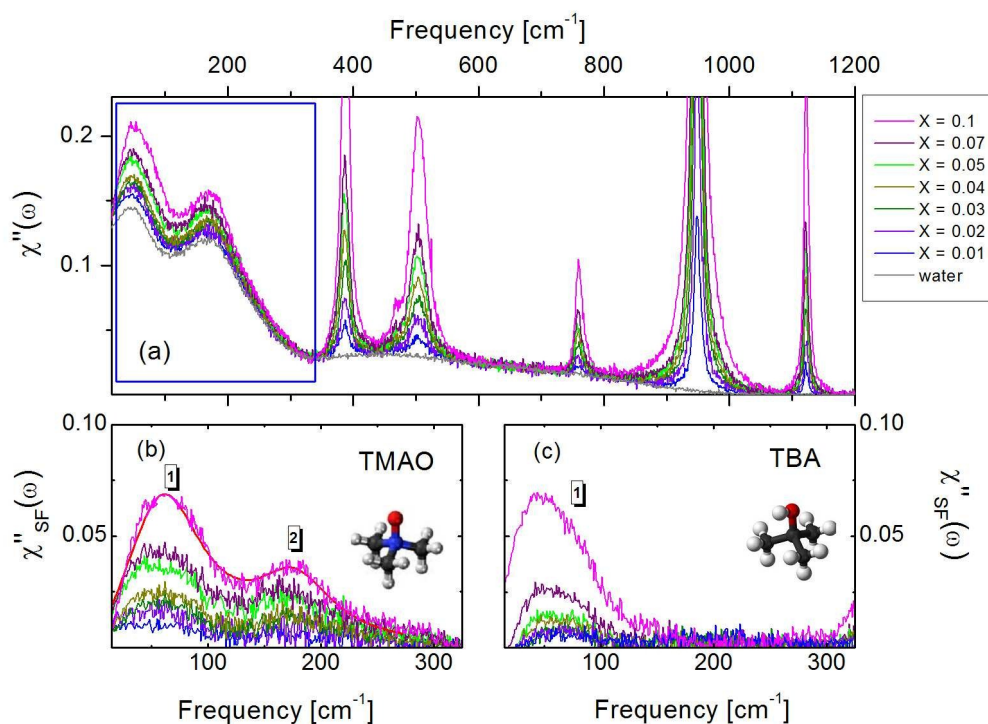


FIG. 5. Panel (a): Low frequency Raman spectra of TMAO aqueous solutions at different concentrations. Panel (b)-(c): Solvent free spectra of TMAO/water and TBA/water mixtures calculated

by subtracting the spectrum of pure water from those of the solutions, reported in the 15-330 cm^{-1} frequency range.

At first glance, in Fig. 5(b) we observe two asymmetric peaks, labeled as 1 and 2 for clarity: the first is located at about 60-70 cm^{-1} , the second at about 180-190 cm^{-1} , and both of them increase with concentration. These peaks can be attributed to direct contributions arising from the solute, or to solute-induced changes on the water signal, or both. Peak 1 is rather typical of liquids;^{65,66,67,68} for anisotropic molecular systems it is generally attributed to hindered rotations (librations) of molecules within the potential cage formed by the solvent.⁶⁷ We have already identified a similar feature in TBA/water solutions (see Fig. 5(c)), which has been attributed to TBA librations. This mode has been found to be sensitive to aggregation of the solute.⁴¹ The position of peak 2 results to be very close to that of the intermolecular stretching mode of pure water. Additional insight is provided by comparison with TBA. When we look at solvent-free Raman spectra of TMAO/water and TBA/water solutions collected at the same concentrations (Figs. 5(b) and 5(c)), two differences capture our attention: as solute concentration increases, the position of peak 1 seems to vary much less in TMAO than in TBA solutions; moreover, peak 2 in TBA is almost missing. This indicates that, despite the similarity in the structure, the difference in hydrophilic moieties of the two systems, which leads to a different strength of hydrogen bonds,^{3,4,15} is reflected in this part of the spectrum.

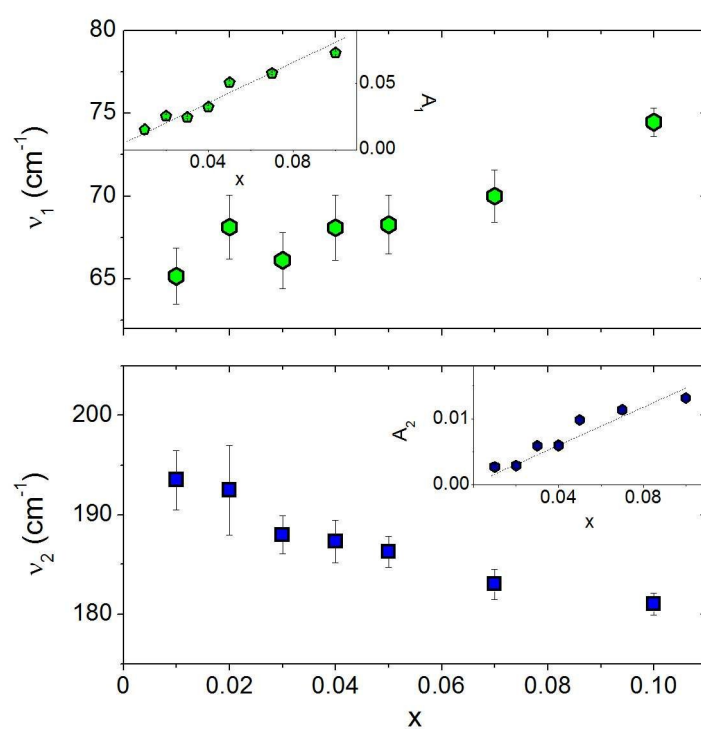


Fig. 6. Dependence on the solute molar ratio of the frequency position (main panel) and intensity (inset) of the two vibrational modes, labeled as 1 and 2 (top and bottom panel, respectively), obtained by analyzing the TMAO solvent-free Raman spectra from 15 to 330 cm^{-1} by using two brownian oscillator functions.

From a quantitative point of view, more information can be gained by following the evolution of the intensity/position of the two peaks over the 15–330 cm^{-1} spectral range as the solute concentration increases. The analysis of χ''_{SF} has been done by using two brownian oscillator functions³⁵ (as an example, the fitting curve for the $x=0.1$ TMAO/water solution is shown as a continuous red line in Fig 5(b)), and the corresponding fitting parameters are shown in Fig. 6. Within the experimental uncertainty, it is clear that the intensity of both vibrational modes increases almost linearly with the solute molar ratio, and the corresponding peak position exhibits a smooth change, the damping parameter (data not shown) being almost constant in both cases. Interestingly, we notice that the frequency position of peak 1 changes almost linearly, in contrast with what found in TBA,⁴¹ where a much greater (more than double) variation of the average peak position was detected, marked by the occurrence of a change in the slope at about $x=0.03$, due to TBA aggregation.

We can therefore argue that the librational modes of TMAO and TBA in the aqueous medium behave very differently, since the molecules experience different environments. A blue-shift of the librational mode of TMAO can be related to a progressive strengthening of intermolecular forces around the solute, while a red-shift was found in the case of TBA.

Concerning peak 2, only present in TMAO/water solutions, we notice that its frequency position progressively decreases as a function of concentration. In pure water this mode, which is collective in nature, is generally related to the presence of ordered H-bonded tetrahedral environments and generally a solute-induced depletion is observed.^{48,69} As already discussed, TMAO can act as H-bond acceptor in the formation of strong H-bonds with up to three water molecules,^{30,70} as recently confirmed by joint Raman experiments and electronic structure computations.^{71,72} In the light of these arguments, peak 2 is tentatively ascribed to an intermolecular stretching mode of water molecules H-bonded to TMAO. This specific intermolecular TMAO-water mode would mainly involve water motions (due to mass effects) and should be peaked at slightly lower frequencies than the stretching mode of water, as it is the case. A relatively larger Raman cross-section would also be expected for this mode. This speculation, however, needs to be verified in more detail and computer simulations may be conclusive with regard to the vibrational assignment of this mode.

We can conclude that the vibrational dynamics of TMAO and TBA in the low-frequency Raman region bears the stamp of their interaction with water. Our results further support the indication that in dilute aqueous solution TBA tends to aggregate and TMAO does not; moreover, probably due to the formation of specific solute-water H-bonds, TMAO is able to modify to a greater extent the vibrational distribution of the low frequency Raman spectrum.

CONCLUSIONS

The effects of hydration on the dynamics of polarisability anisotropy fluctuations in TMAO/water solutions have been investigated by using EDLS spectroscopy. The wide frequency range accessed by this technique has allowed us to obtain information about TMAO and water properties, simultaneously. Two water populations have been identified, hydration and bulk water, which relax through a restructuring of the H-bond network via translational processes at the picosecond timescale. Of these populations, the former is found to be dynamically retarded with respect to the latter by a factor 4. Such a retardation factor equals that found in TBA/water solutions, but is smaller than that revealed in a number of systems, including sugars, peptides, aminoacids, and proteins,^{33,34,36,37,53} indicating that hydrophobic groups in TBA and TMAO have a greater impact than the hydrophilic portion of these molecules on the picosecond relaxation water dynamics. Like in TBA, the spatial extent of the perturbation induced by TMAO on surrounding water is found to be short-ranged, and limited to the first hydration shell, differently from more complex amphiphiles, where the perturbation extends up to three or more hydration layers.^{35,36,37,38} Overall, the similarly small retardation factor, and small number of water molecules perturbed by each solute molecule in TMAO and TBA,⁴¹ as obtained by EDLS, are in favor of the idea that hydrophobic hydration is less effective in modifying the H-bond network of liquid water. Like in TBA, a decreasing hydration number has been observed, mostly arising from changes near the methyl groups. In the case of TMAO, however, this behavior can be fully explained by a finite probability of finding solute molecules in a close-to-contact condition; in the other case, a steeper concentration dependence reveals a tendency of TBA molecules to self-aggregate. The higher propensity for TMAO with respect to TBA to form solute-water hydrogen bonds is likely to disadvantage episodes of aggregation in the former.

These findings are confirmed by the collective vibrational dynamics in the THz frequency region (from tens to several hundreds of cm^{-1}). In the presence of TMAO, two bands are observed in the solvent-free spectra, peaked at about 60 and 170 cm^{-1} , which maintain at all

concentrations the characteristic features of a monomeric aqueous dispersion, confirming the absence of hydrophobic aggregation among solute molecules. In the TBA solution, with increasing concentration, the first peak moves to lower frequencies, towards the frequency value measured in pure TBA, as expected for solute molecules that cluster into bigger and bigger aggregates; the second peak is missing.

As a whole, EDLS results prove that in diluted solutions: i) TBA tends to aggregate and TMAO does not; ii) TMAO modifies more strongly than TBA the collective tetrahedral structure of water, possibly because of a higher ability to form solute-water hydrogen bonds. More generally, we provide a methodology to analyze a great number of properties related to solvation and aggregation phenomena in biosystem solutions, which can be extended to the study of ternary mixtures, so relevant in the field of biomolecular stability.

We conclude our considerations by pointing out several critical questions that hopefully will be clarified in the near future: First, the present EDLS results indicate that the lifetime of TMAO-water aggregates is short (<20 ps), at odds with the description adopted in Ref. 30 for dielectric spectra, where it turns out to be much longer (>50 ps). Moreover, the present low-frequency Raman spectra show a signal that we are tentatively connecting to the intermolecular stretching mode of water molecules H-bonded to TMAO, but this assignment needs a definitive proof. Finally, the behavior of hydration numbers as a function of concentration derived by EDLS suggests a propensity of TBA molecules to self-aggregate (above a certain concentration in water solution);⁴¹ this offers a somewhat different view from that proposed in recent works^{5,60} where the occurrence of solute-solute contacts in TBA solutions is instead essentially random.

ACKNOWLEDGEMENTS

S.C. acknowledges support from MIUR-PRIN (Project 2012J8X57P). M.P. acknowledges support from MIUR-PRIN 2010–2011.

† Electronic supplementary information (ESI) available: Relaxations contributions of Hydration and Bulk Water

REFERENCES

- ¹ P. Ball, *Chem. Rev.*, 2008, **108**, 74–108.
- ² J. G. Davis, K. P. Gierszal, P. Wang and D. Ben-Amotz, *Nature*, 2012, **491**, 582–585.
- ³ A. Di Michele, M. Freda, G. Onori, M. Paolantoni, A. Santucci and P. Sassi, *J. Phys. Chem. B*, 2006, **110**, 21077–21085.
- ⁴ R. Sinibaldi, C. Casieri, S. Melchionna, G. Onori, A. L. Segre, S. Viel, L. Mannina and F. De Luca, *J. Phys. Chem. B*, 2006, **110**, 8885–8892.
- ⁵ D. S. Wilcox, B. M. Rankin and D. Ben-Amotz, *Faraday Discuss.*, 2013, **167**, 177.
- ⁶ B. M. Rankin, D. Ben-Amotz, Dor, S. T. Van der Post, H. J. Bakker, *J. Phys. Chem. Lett.*, **6**, 688, 2015.
- ⁷ A. Fiore, V. Venkateshwaran and S. Garde, *Langmuir*, **29**, 2013, 8017.
- ⁸ C. C. Mello and D. Barrick, *Protein Sci.*, 2003, **12**, 1522.
- ⁹ J. Ma, I. M. Pazos and F. Gai, *Proc. Natl. Acad. Sci. USA*, 2014, **111**, 8476–8481.
- ¹⁰ F. Meersman, D. Bowron, A. K. Soper and M. H. J. Koch, *Biophys. J.*, 2009, **97**, 2559–2566.
- ¹¹ G. Graziano, *Phys. Chem. Chem. Phys.*, 2012, **14**, 13088–13094.
- ¹² F. Franks, in: F. Franks (Ed.), *Water: a Comprehensive Treatise*, vol. 2, Plenum, New York, 1974 (chap. 1); F. Franks, D.S. Reid, in: F. Franks (Ed.), *Water: a Comprehensive Treatise*, vol. 2, Plenum, New York, 1974 (chap. 5); F. Franks, in: F. Franks (Ed.), *Water: a Comprehensive Treatise*, vol. 4, Plenum, New York, 1975 (chap. 1, and references therein).
- ¹³ C. Petersen, A. A. Bakulin, V. G. Pavelyev, M. S. Pshenichnikov and H. J. Bakker, *J. Chem. Phys.* 2010, **133**, 164514.
- ¹⁴ D. Laage, G. Stirnemann and J. T. Hynes, *J. Phys. Chem. B*, 2009, **113**, 2428–2435.
- ¹⁵ S. Paul and G.N. Patey, *J. Phys. Chem. B*, 2006, **110**, 10514.
- ¹⁶ M. Montagna, F. Sterpone and L. Guidoni, *J. Phys. Chem. B*, 2012, **116**, 11695.
- ¹⁷ A. K. Soper and J. L. Finney, *Phys. Rev. Lett.*, 1993, **71**, 4346.
- ¹⁸ F. Meersman, D. Bowron, A. K. Soper and M. H. J. Koch, *Biophys. J.*, 2009, **97**, 2559–2566.
- ¹⁹ A. A. Bakulin, M. S. Pshenichnikov, H. J. Bakker and C. Petersen, *J. Phys. Chem. A*, 2011, **115**, 1821–1829.
- ²⁰ K.-J. Tielrooij, J. Hunger, R. Buchner, M. Bonn and H. J. Bakker, *J. Am. Chem. Soc.*, 2010, **132**, 15671–15678.
- ²¹ J. T. Titantah and M. Karttunen, *J. Am. Chem. Soc.*, 2012, **134**, 9362–9368.
- ²² M. Nakahara, C. Wakai, Y. Yoshimoto and N. Matubayasi, *J. Phys. Chem.*, 1996, **100**, 1345–1349.
- ²³ Y. Ishihara, S. Okouchi and H. Uedaira, *Faraday Trans.*, 1997, **93**, 3337–3342.
- ²⁴ J. Qvist and B. Halle, *J. Am. Chem. Soc.*, 2008, **130**, 10345–10353.
- ²⁵ L. Lupi, L. Comez, C. Masciovecchio, A. Morresi, M. Paolantoni, P. Sassi, F. Scarponi and D. Fioretto, *J. Chem. Phys.*, 2011, **134**, 055104.
- ²⁶ L. Comez, L. Lupi, M. Paolantoni, F. Picchiò and D. Fioretto, *J. Chem. Phys.*, 2012, **137**, 114509.
- ²⁷ M. Freda, G. Onori and A. Santucci, *J. Mol. Struct.*, 2001, **153**, 565–566.
- ²⁸ Y. L. A. Rezus and H. J. Bakker, *Phys. Rev. Lett.*, 2007, **99**, 148301.
- ²⁹ Y. L. A. Rezus and H. J. Bakker, *J. Phys. Chem. B*, 2009, **113**, 4038.
- ³⁰ J. Hunger, K.-J. Tielrooij, R. Buchner, M. Bonn and H. J. Bakker, *J. Phys. Chem. B*, 2012, **116**, 4783–4795.
- ³¹ K. Mazur, I. A. Heisler and S. R. Meech, *J. Phys. Chem. B*, 2011, **115**, 2563–2573.
- ³² K. Mazur, I. A. Heisler and S. R. Meech, *Phys. Chem. Chem. Phys.*, 2012, **14**, 6343–6351.
- ³³ M. Paolantoni, L. Comez, M.E. Gallina, P. Sassi, F. Scarponi, D. Fioretto and A. Morresi, *J. Phys. Chem. B*, 2009, **113**, 7874.

- ³⁴ L. Lupi, L. Comez, M. Paolantoni, S. Perticaroli, P. Sassi, A. Morresi, B. M. Ladanyi and D. Fioretto, *J. Chem. Phys.*, 2012, **116**, 14760-14767.
- ³⁵ S. Perticaroli, L. Comez, M. Paolantoni, P. Sassi and A. Morresi, *J. Am. Chem. Soc.*, 2011, **133**, 12063.
- ³⁶ L. Comez, L. Lupi, A. Morresi, M. Paolantoni, P. Sassi and D. Fioretto, *J. Phys. Chem. Lett.*, 2013, **4**, 1188-1192.
- ³⁷ L. Comez, S. Perticaroli, M. Paolantoni, P. Sassi, S. Corezzi, A. Morresi and D. Fioretto, *Phys. Chem. Chem. Phys.*, 2014, **16**, 12433.
- ³⁸ S. Perticaroli, L. Comez, M. Paolantoni, P. Sassi, L. Lupi, D. Fioretto, A. Paciaroni and A. Morresi, *J. Phys. Chem. B*, 2010, **114**, 8262.
- ³⁹ S. Perticaroli, L. Comez, P. Sassi, M. Paolantoni, S. Corezzi, S. Caponi, A. Morresi and D. Fioretto, *J. Non Cryst-Solids*, 2015, **407**, 472-477.
- ⁴⁰ S. Perticaroli, D. Russo, M. Paolantoni, M. A. Gonzalez, P. Sassi, J. D. Nickles, L. Comez, E. Pellegrini, D. Fioretto and A. Morresi, *Phys. Chem. Chem. Phys.*, 2015, **17**, 11423-11431.
- ⁴¹ L. Comez, M. Paolantoni, L. Lupi, P. Sassi, S. Corezzi, A. Morresi and D. Fioretto; *J. Phys. Chem. B*, 2015, **119**, 9236.
- ⁴² L. Comez, C. Masciovecchio, G. Monaco and D. Fioretto, Progress in Liquid and Glass Physics by Brillouin Scattering Spectroscopy. In *Solid State Physics*; Elsevier, 2012; Vol. **63**, pp. 1-77.
- ⁴³ A. Sokolov, J. Hurst and D. Quitmann, *Phys. Rev. B*, **51**, 1995, 12865-12868.
- ⁴⁴ M. Paolantoni, P. Sassi, A. Morresi and S. Santini, *J. Chem. Phys.*, **127**, 2007, 024504.
- ⁴⁵ M. D. Elola and B. M. Ladanyi, *J. Chem. Phys.*, **126**, 2007, 084504.
- ⁴⁶ M. T. Sonoda, S. R. M. Vechi and M. S. Skaf, *Phys. Chem. Chem. Phys.*, **7**, 2005, 1176.
- ⁴⁷ O. Faurskov Nielsen, *Annu. Rep. Prog. Chem., Sect. C*, **93**, 1997, 57-99.
- ⁴⁸ B. Rossi, L. Comez, L. Lupi, S. Caponi and F. Rossi, *Food Biophys.*, **6**, 2011, 227.
- ⁴⁹ S. Corezzi, P. Sassi, M. Paolantoni, L. Comez, A. Morresi and D. Fioretto, *J. Chem. Phys.*, **140**, 2014, 184505.
- ⁵⁰ D. Fioretto, L. Comez, M. E. Gallina, A. Morresi, L. Palmieri, M. Paolantoni, P. Sassi and F. Scarponi, *Chemical Physics Letters*, **441**, 2007, 232-236.
- ⁵¹ M. E. Gallina, L. Comez, A. Morresi, M. Paolantoni, S. Perticaroli, P. Sassi and D. Fioretto, *J. Chem. Phys.*, **132**, 2010, 214508.
- ⁵² R. Torre, P. Bartolini and R. Righini, *Nature*, **428**, 2004, 296-299.
- ⁵³ L. Lupi, L. Comez, M. Paolantoni, D. Fioretto and B. M. Ladanyi, *J. Phys. Chem. B*, **116**, 2012, 7499-7508
- ⁵⁴ M. Paolantoni, L. Comez, D. Fioretto, M.E. Gallina, A. Morresi, P. Sassi and F. Scarponi, *J. Raman Spect.*, **39**, 2008, 238.
- ⁵⁵ L. Lupi, L. Comez, M. Paolantoni, P. Sassi, A. Morresi and D. Fioretto; contribution to a volume "Sucrose: Properties, Biosynthesis and Health Implications" NOVA Editions. Series: Food Science and Technology Biochemistry Research Trend Pub: 2013- March ISBN: 978-1-62417-984-6).
- ⁵⁶ B. Rossi, L. Comez, D. Fioretto, L. Lupi, S. Caponi and F. Rossi, *J. Raman Spect.*, **42**, 2011, 1479.
- ⁵⁷ G. Stirnemann, F. Sterpone and D. Laage, *J. Phys. Chem. B*, **115**, 2011, 3254-3262.
- ⁵⁸ D. Fioretto, L. Comez, S. Corezzi, M. Paolantoni, P. Sassi and A. Morresi, *Food Biophysics*, **8**, 2013, 177-182.
- ⁵⁹ A. Fornili, M. Civera, M. Sironi and S. L. Fornili, *Phys. Chem. Chem. Phys.*, **5**, 2003, 4905.
- ⁶⁰ B. M. Rankin, B. M., D. Ben-Amotz, Dor, S. T. Van der Post and H. J. Bakker, *J Phys. Chem. Lett*, **6**, 2015, 688.
- ⁶¹ S. Arrhenius, *Biochem. J.* **11**, 1917, 112.
- ⁶² D. Kivelson and P. A. Madden, *Annu. Rev. Phys. Chem.*, **31**, 1980, 523-558.
- ⁶³ M. Freda, G. Onori and A. Santucci, *J. Mol. Struct.*, **565-566**, 2001, 153-157.

-
- ⁶⁴T. Shikata and S. J. Itatani, *Solution Chem.*, **31**, 2002, 823.
- ⁶⁵F. Palombo, P. Sassi, M. Paolantoni, C. Barontini, A. Morresi and M. G. Giorgini, *J. Phys. Chem. B*, **118**, 2014, 215.
- ⁶⁶N. T. Hunt, A. R. Turner and K. Wynne, *J. Phys. Chem. B*, **109**, 2005, 19008–19017.
- ⁶⁷P. Sassi, M. Paolantoni, S. Perticaroli, F. Palombo and A. Morresi, *J. Raman Spectrosc.*, **40**, 2009, 1279–1283.
- ⁶⁸N. A. Smith and S. R. Meech, *Faraday Disc.*, **108**, 1997, 35–50.
- ⁶⁹S. Perticaroli, P. Sassi, A. Morresi and M. Paolantoni, *J. Raman Spectrosc.*, **39**, 2008, 227–232.
- ⁷⁰G. Stirnemann, J. T. Hynes and D. Laage, *J. Phys. Chem. B*, **114**, 2010, 3052–3059.
- ⁷¹K. L. Munroe, D. H. Magers and N. I. Hammer, *J. Phys. Chem. B*, **115**, 2011, 7699–7707.
- ⁷²K. A. Cuellar, K. L. Munroe, D. H. Magers and N. I. Hammer, *J. Phys. Chem. B*, **118**, 2014, 449–459.